

# Thermochemical and Spectroscopic Studies of Chemically Vapor-Deposited Amorphous Silica

Maria Huffman\* and Alexandra Navrotsky

Department of Chemistry, Arizona State University, Tempe, Arizona 85287

Fabio S. Pintchovski\*

Motorola, Incorporated, Advanced Product Research and Development Laboratories, Austin, Texas 78721

## ABSTRACT

Two kinds of low pressure CVD SiO<sub>2</sub> samples, heterogeneous film and homogeneous "snow," have been collected on stainless steel substrates at three different deposition temperatures: 523, 643, and 703 K. They have been characterized thermodynamically by transposed temperature drop and high temperature solution calorimetry. Both film and "snow" samples are metastable—in terms of enthalpy relative to bulk SiO<sub>2</sub> glass—by up to 101 kJ·mol<sup>-1</sup>. The excess enthalpy increases with decreasing deposition temperature and is larger for "snows" than for films. On annealing at high temperatures, it gradually disappears. IR and Raman spectroscopies indicate that both Si-H and Si-OH species are present in the as-deposited samples but disappear upon annealing. All as-deposited samples have densities comparable to bulk SiO<sub>2</sub> glass, *i.e.*, between 2.0 and 2.2 g·cm<sup>-3</sup>. Annealing tends to increase the density of all samples.

Various doped silica glasses (SiO<sub>2</sub>-P<sub>2</sub>O<sub>5</sub>, SiO<sub>2</sub>-B<sub>2</sub>O<sub>3</sub>, SiO<sub>2</sub>-As<sub>2</sub>O<sub>3</sub> etc., with dopant concentrations of up to 20 mole percent) are widely used in the semiconductor industry either as dielectrics (1) or as final passivation layers (2, 3). One of the major methods of obtaining these glasses as thin films is low pressure chemical vapor deposition (LPCVD) (4). Two kinds of amorphous sample can be obtained from a hot wall LPCVD furnace: thin films heterogeneously deposited on the substrate in the central hot zone and homogeneously deposited reactive powder adhering to the furnace walls at the cooler ends of the deposition tube. The term "snow" will be used throughout this paper as a common name describing these powdery SiO<sub>2</sub> CVD deposits.

Since the basis of many doped-glass systems is SiO<sub>2</sub>, calorimetric and spectroscopic studies have been carried out on both thin film and snow LPCVD SiO<sub>2</sub>. High temperature calorimetry has been utilized to obtain thermodynamic data. Scanning electron microscopy and IR and Raman spectroscopies (5) have been used for structural characterization. This paper will show that significant differences in energetics, structure, and properties exist between low temperature-deposited SiO<sub>2</sub> and normal bulk SiO<sub>2</sub> glass. The main focus of this study is on a general understanding of the variation of properties of CVD SiO<sub>2</sub> over a wide range of preparation and annealing conditions, rather than on the optimization of properties over a smaller range of processing conditions used by the semiconductor industry.

## Experimental

**LPCVD and annealing.**—All samples were prepared using a standard LPCVD system. In this study, ~0.4-0.5 mm thick stainless steel wafers, of 100 mm diam, were used as substrates, enabling the deposited film to be peeled off the wafer by a simple bending motion. The wafers stood vertically, facing the ends of the deposition tube. The wafer spacing was typically 3-5 mm. Both films and snows were obtained in a single run. In the apparatus used, the input gas flow rates were measured and controlled by rotameter-type flowmeters. The gases used were SiH<sub>4</sub> and O<sub>2</sub>, which react in the hot reaction chamber to produce amorphous solid SiO<sub>2</sub>. The deposition parameters are listed in Table I. Each run was approximately 20h long, producing SiO<sub>2</sub> films 3-5 μm thick. Five stainless steel wafers were used in each run for film collection. The amount of film obtained was less than 1 g/run. Thin film SiO<sub>2</sub> was obtained at 523, 643, and 703 K. Snow SiO<sub>2</sub> was obtained at the same furnace temperatures but at the colder ends of the CVD furnace. Thus, in

the 523 K furnace run, snow was obtained from a range of 327-455 K; in the 643 K furnace run, it was obtained from 419 to 533 K, and, in the 703 K run, from 344 to 673 K. The samples were analyzed for purity by flame photometry. Metallic impurities were found ranging from 6 to about 1500 ppm (see Table II). Most of the impurities in the films came from the stainless steel substrate.

Films and snows were placed in alumina crucibles in small quantities (20-50 mg) and were annealed for two or three days at temperatures ranging from 773 to 1223 K. These samples, in addition to the as-deposited ones, were used in drop and solution calorimetry and were also examined spectroscopically, by scanning electron microscopy, and by density measurements.

**High temperature calorimetry.**—The calorimeter used for obtaining thermodynamic data at 973 K is of the Tian-Calvet type and has been described elsewhere (6). Two types of experiment were performed. The first is "transposed temperature drop" calorimetry, in which a sample of CVD SiO<sub>2</sub>, encapsulated in Pt, is dropped from room temperature into the hot calorimeter. During this first drop, the sample heats to 973 K and releases any stored energy that can be annealed quickly at that temperature. The sample is then retrieved, and the drop experiment is repeated. The second drop gives the heat content of the

Table I. Deposition parameters for the LPCVD experiments

Temperature of deposition (K)	SiH <sub>4</sub> flow (cm <sup>3</sup> /min)	O <sub>2</sub> flow (cm <sup>3</sup> /min)	Pressure (mtorr)	Deposition rate (nm/min) <sup>a</sup>
523	84	94	400 ± 50	6
643	84	94	400 ± 50	19
703	84	94	400 ± 50	17

<sup>a</sup> Initial deposition rate calculated from 15-20 min test runs. It drops drastically after the first hour of deposition, leading to much thinner deposits than one would otherwise expect after 20h.

Table II. Impurities present in the CVD snow and film samples

Impurity (metal)	Impurity content (ppm)	
	Snows	Films
Ca	≤20	—
Mg	5 ± 3	140 ± 30
Al	11 ± 8	—
Fe	60 ± 20	1300 ± 200
Ti	≤150	≤500
Cr	—	1500 ± 500
Mn	—	280 ± 30

\*Electrochemical Society Active Member.

annealed sample. The difference between the first drop and the second drop gives the enthalpy (at room temperature) of any annealing process or phase transition that occurs rapidly at 973 K. The second type of experiment is solution calorimetry using molten  $2\text{PbO} \cdot \text{B}_2\text{O}_3$  at 973 K. The sample (10–30 mg) is thermally equilibrated at 973 K and then dissolved completely in the oxide melt. Its heat of solution can be compared to that of bulk  $\text{SiO}_2$  glass, in order to measure the stored energy that does not anneal rapidly at 973 K but is released when the sample is dissolved. The experimental details have been described previously (6).

**Density measurements.**—The densities of all CVD film samples grown on stainless steel wafers were obtained by pycnometry. The heavy liquid used was perfluoro-1-methyldecalin.<sup>1</sup> Small amounts of sample (10–50 mg) were placed in a cup and weighed—first in air and then in the heavy liquid—on a Sartorius 2434 semimicrobalance. The liquid was calibrated using a high purity Si single crystal as a standard (density  $2.33 \text{ g}\cdot\text{cm}^{-3}$ ). The density of the snow samples could not be measured accurately, owing to the samples' high porosity. Furthermore, measurements of the refractive indexes of the snows were attempted using a microscope and immersion oils. The results were too variable for direct comparison with those of the films.

For comparison, the densities of CVD  $\text{SiO}_2$  films deposited on Si wafers at deposition temperatures of 523, 643, and 703 K were also measured. Clean, (100) p-type boron-doped Si wafers with resistivities of 40–50  $\Omega\cdot\text{cm}$  were weighed and then used as substrates for  $\text{SiO}_2$  deposition. After the deposition runs, the wafers were weighed again, thus providing the amount of deposited  $\text{SiO}_2$ . The thickness of the films was measured, and the densities were calculated from the weight-volume ratios. Thickness and refractive index measurements were made simultaneously using a Metricon 2000 prism coupler.<sup>2</sup> These measurements could not be done directly on  $\text{SiO}_2$  films deposited on stainless steel wafers because of the roughness of the substrate. Since the stainless steel wafers were etched before deposition, cracks developed and  $\text{SiO}_2$  film deposited unevenly on the substrate surface, making it very difficult to measure the thickness and the refractive index of the CVD layer.

In order to investigate the effects of annealing on densities and refractive indexes, these properties were measured for annealed  $\text{SiO}_2$  CVD films grown on stainless steel and Si wafers. The annealing time in air was 72h at 773, 873, 973, and 1173 K. The reason for choosing such a long anneal will be evident from the discussion on thermodynamics in the following section. In brief, short anneals (1/2h or less at 973 K) cause a considerable decrease in the excess stored energy in the CVD samples (drop calorimetry). However, only long anneals (~3 days at

1173–1223 K) ensure complete loss of Si-OH and Si-H species and energetic stability (excess stored energy close to zero).

**Infrared and Raman spectroscopy.**—A Nicolet MX-1 FT-IR spectrometer was used for obtaining the infrared spectra. Approximately 1 mg of sample was ground with ~115 mg of KBr and pelletized. The disks were then placed in a drying oven at 373 K for about 24h. Raman spectra were run with an Instruments S.A. U-1000 double monochromator system, using either the 488.0 nm or the 514.5 nm line of a Coherent Innova 90-4 argon laser. Details have been given previously (5).

**Scanning electron microscopy (SEM).**—An ISI-SS40 scanning electron microscope was used for obtaining SEM micrographs of all the samples. The samples, after mounting, were coated with gold to avoid charging problems.

## Results and Discussion

**High temperature calorimetry.**—The results of drop calorimetry are shown in Table III. For both film and snow samples, the heat effect seen on the first drop is less endothermic than that for subsequent (second and third) drops, implying a rapid release of energy on the first anneal at 973 K. For the snows prepared at 419–533 and 327–495 K, this effect is so large that the first drop actually has a net exothermic heat effect. The magnitude of the heat released, when compared to bulk  $\text{SiO}_2$  glass, ranges from 15 to 101  $\text{kJ}\cdot\text{mol}^{-1}$ . On the second and third drops, the heat content of film and snow samples is similar to that of bulk silica glass ( $41.9 \text{ kJ}\cdot\text{mol}^{-1}$ ) (7).

The results of solution calorimetry are shown in Table IV. Despite some scatter in the data, it is clear that the heat of solution becomes progressively less exothermic upon annealing and approaches that of bulk  $\text{SiO}_2$  glass. Annealing above 1223 K causes the onset of crystallization, as observed by means of optical microscopy.

The thermodynamic data show that the LPCVD  $\text{SiO}_2$  samples are very metastable, in terms of enthalpy, relative to bulk  $\text{SiO}_2$  glass. This excess enthalpy can be annealed out gradually by heating. At 973 K, some of the stored enthalpy is released rapidly (by a drop experiment), and some is released only when the sample is dissolved. This suggests that more than one mechanism for storing excess energy may be involved. It is possible that the rapidly released energy reflects changes in bond angles, and the energy released on dissolution may reflect differences in ring size and bonding arrangements, differences that would require the breaking of Si-O bonds.

Table IV. Solution calorimetry results

Sample	Deposition T (K)	Anneal T (K)	t (h)	$\Delta H_{\text{sol}}$ $\text{kJ}\cdot\text{mol}^{-1}$
Snow	344-673	973	20	$-43.60 \pm 0.59^a$ (2) <sup>b</sup>
Snow	344-673	1123	20	$-36.05 \pm 1.04$ (2)
Snow	344-673	1123	72	$-35.77 \pm 1.30$ (2)
Snow	344-673	1223	20	$-30.28 \pm 1.10$ (2)
Snow	344-673	1223	72	$-30.11 \pm 1.15$ (2)
Snow <sup>c</sup>	419-533	973	20	$-11.63$ (1)
Snow <sup>d</sup>	419-533	973	20	$-9.73 \pm 1.68$ (2)
Snow	327-455	973	20	$-9.48 \pm 0.68$ (2)
Snow	327-455	1123	24	$-12.62 \pm 1.15$ (2)
Snow	327-455	1123	72	$-12.97$ (1)
Snow	327-455	1223	24	$-10.84 \pm 1.53$ (2)
Snow	327-455	1223	72	$-11.11 \pm 1.92$ (2)
Film	703	973	20	$-14.06 \pm 0.30$ (2)
Film	703	1173	48	$-10.34 \pm 0.77$ (2)
Film	643	973	65	$-21.74 \pm 0.33$ (2)
Film	643	1173	67	$-17.11$ (1)
Film	523	973	20	$-12.22 \pm 1.95$ (2)
Bulk glass	—	—	—	$-11.30 \pm 0.21$ (4)

<sup>1</sup>Columbia Organic Chemicals, Incorporated, Columbia, South Carolina 29290.

<sup>2</sup>Metricon Corporation, Pennington, New Jersey 08534.

Table III. Drop calorimetry results

Drop	Deposition T(K)		Snow $\text{SiO}_2$ $H_{973} - H_{298}$ ( $\text{kJ}\cdot\text{mol}^{-1}$ )	Film $\text{SiO}_2$ $H_{973} - H_{298}$ ( $\text{kJ}\cdot\text{mol}^{-1}$ )
	Snow	Film		
1	344-673	703	$27.20 \pm 0.18^a$ (2) <sup>b</sup>	$22.53 \pm 0.28$ (2)
2	344-673	703	$42.01 \pm 0.65$ (2)	$40.94 \pm 0.38$ (2)
3	344-673	703	$41.54 \pm 1.19$ (3)	$42.55$ (1)
1	419-533	643	$-36.80 \pm 2.33$ (2)	$19.06 \pm 0.03$ (2)
			$-61.51 \pm 3.75$ (4) <sup>c</sup>	
2	419-533	643	$39.88 \pm 2.37$ (2)	$40.40 \pm 1.27$ (2)
			$38.55 \pm 0.76$ (2) <sup>d</sup>	
1	327-455	523	$-19.79 \pm 1.48$ (2)	$-1.02 \pm 1.06$ (2)
2	327-455	523	$39.94 \pm 2.57$ (2)	$39.12 \pm 1.60$ (2)

<sup>a</sup>  $\pm 1\sigma$ .

<sup>b</sup> Number of successful experiments.

<sup>c, d</sup> Two batches of snow sample from two separate but nominally identical LPCVD runs.

<sup>a</sup>  $\pm 1\sigma$ .

<sup>b</sup> Number of successful experiments.

<sup>c, d</sup> Two batches of snow sample from two separate but nominally identical LPCVD runs.

Table V. Enthalpy differences between CVD SiO<sub>2</sub> and bulk silica glass

Type of sample	Preparation T (K)	Anneal		Enthalpy difference		Total excess enthalpy (kJ·mol <sup>-1</sup> )
		T (K)	t (h)	(Drop) (kJ·mol <sup>-1</sup> )	(Solution) (kJ·mol <sup>-1</sup> )	
Film	703	—	—	19.35 ± 0.28 <sup>a</sup>	2.76 ± 0.37 <sup>b</sup>	22.11 ± 0.46 <sup>c</sup>
Film	703	973	20	0	2.76 ± 0.37	2.76 ± 0.37
Film	703	1173	48	0	-0.97 ± 0.80	-0.97 ± 0.80
Film	643	—	—	22.82 ± 0.03	10.44 ± 0.39	33.26 ± 0.39
Film	643	973	65	0	10.44 ± 0.31	10.44 ± 0.31
Film	643	1173	67	0	5.81 ± 0.21	5.81 ± 0.21
Film	523	—	—	42.90 ± 1.06	0.92 ± 1.96	43.82 ± 2.23
Film	523	973	20	0	0.92 ± 1.96	0.92 ± 1.96
Snow	344-673	—	—	14.68 ± 0.18	32.30 ± 0.63	46.98 ± 0.66
Snow	344-673	973	20	0	32.30 ± 0.63	32.30 ± 0.63
Snow	344-673	1123	20	0	24.75 ± 1.06	24.75 ± 1.06
Snow	344-673	1123	72	0	24.47 ± 1.32	24.47 ± 1.32
Snow	344-673	1223	20	0	18.98 ± 1.12	18.98 ± 1.12
Snow	344-673	1223	72	0	18.81 ± 1.17	18.81 ± 1.17
Snow	419-533	—	—	78.68 ± 2.33	0.33 ± 0.21	79.01 ± 2.34
Snow	419-533	973	20	0	0.33 ± 0.21	0.33 ± 0.21
Snow	419-533	—	—	103.39 ± 3.75	-1.57 ± 1.69	101.82 ± 4.11
Snow	419-533	973	20	0	-1.57 ± 1.69	-1.57 ± 1.69
Snow	327-455	—	—	61.67 ± 1.48	-1.82 ± 0.71	59.85 ± 1.64
Snow	327-455	973	20	0	-1.82 ± 0.71	-1.82 ± 0.71
Snow	327-455	1123	24	0	1.32 ± 1.17	1.32 ± 1.17
Snow	327-455	1123	72	0	1.67 ± 0.21	1.67 ± 0.21
Snow	327-455	1223	24	0	-0.46 ± 1.54	-0.46 ± 1.54
Snow	327-455	1223	72	0	-0.19 ± 1.93	-0.19 ± 1.93

<sup>a</sup> Errors propagated from drop experiments.

<sup>b</sup> Errors propagated from solution experiments.

<sup>c</sup> Error calculated by propagation of errors of a and b.

Even though the appropriate criterion for stability at constant temperature and pressure is provided by the Gibbs free energy change, the concept of metastability in terms of enthalpy is used here because the  $T\Delta S$  term in the Gibbs free energy function associated with the annealing process is unlikely to overcome the very large negative enthalpy changes observed in the calorimetric experiments.

The total stored excess enthalpy (relative to bulk SiO<sub>2</sub> glass) is the sum of the excess enthalpy in the drop and in the solution experiments (Table V). This is plotted in Fig. 1 as a function of annealing temperature. A series of

curves, one for each initial preparation temperature, is shown. The snows appear to be more metastable than the films, and the lower temperature samples are generally more metastable than the higher temperature ones. On annealing, all the samples, with the exception of the snow deposited during the 703 K LPCVD run, tend to approach bulk silica glass energetically. No explanation for the deviation observed in that particular snow is available. When the total excess enthalpy of the as-deposited samples is plotted as a function of temperature of deposition (see insert in Fig. 1), snow and film samples, except for the 419-533 K snows, fall on a smooth trend when the temperature of deposition of the snows is taken to be the average of the actual range of temperatures from which each sample was obtained. Two batches of snow deposited at 419-533 K (hot zone of the CVD furnace at 643 K) were obtained in separate experiments, in order to compare two nominally identical runs. Both show deviation from the general trends and appear to be the most metastable samples produced (Table V). These samples differ significantly in the heat effect seen on the first drop (Table III), suggesting possible inhomogeneity. Per-

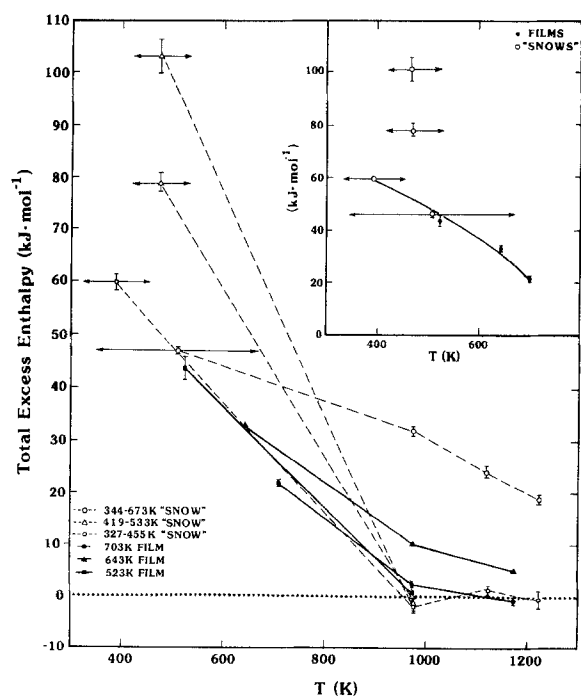


Fig. 1. Total excess enthalpy (kJ mol<sup>-1</sup>) of the snow or film samples compared to bulk SiO<sub>2</sub> glass as a function of annealing temperature. Insert shows total excess enthalpy of as-deposited film and snow samples as a function of deposition temperature. Solid lines are for the films and dashed lines for the snows. Total length of vertical error bars is 2 $\sigma$ . Horizontal error bars indicate range of deposition temperature for snows.

Table VI. Densities and refractive indexes of LPCVD SiO<sub>2</sub> films deposited on Si wafers

Deposition T (K)	Anneal <sup>a</sup> T (K)	Density (g·cm <sup>-3</sup> )	Refractive index
523	—	2.08 ± 0.07 <sup>b</sup> (18) <sup>c</sup>	1.4573 ± 0.0012 <sup>d</sup> (12) <sup>c</sup>
	773	2.09 ± 0.04 (3)	1.4492 ± 0.0002 (5)
	873	2.08 ± 0.02 (3)	1.4519 ± 0.0006 (11)
	973	2.20 ± 0.10 (3)	1.4548 ± 0.0005 (3)
	1173	2.42 ± 0.02 (3)	1.4570 ± 0.0011 (4)
643	—	2.05 ± 0.01 (10)	1.4514 ± 0.0026 (15)
	773	—	1.4513 ± 0.0006 (3)
	873	2.08 ± 0.07 (2)	1.4540 ± 0.0007 (4)
	973	2.02 ± 0.08 (3)	1.4547 ± 0.0008 (3)
	1173	2.56 ± 0.02 (2)	1.4569 ± 0.0009 (3)
703	—	1.99 ± 0.02 (10)	1.4509 ± 0.0012 (22)
	773	—	1.4510 ± 0.0006 (3)
	873	2.09 ± 0.05 (6)	1.4541 ± 0.0014 (6)
	973	2.14 ± 0.06 (6)	1.4555 ± 0.0012 (6)
	1173	2.44 ± 0.10 (4)	1.4570 ± 0.0010 (5)

<sup>a</sup> Each sample annealed in air for 72h.

<sup>b</sup> ± 1 $\sigma$ .

<sup>c</sup> Number of measurements.

<sup>d</sup> ± 3 $\sigma$ .

Table VII. Densities of LPCVD SiO<sub>2</sub> films deposited on stainless steel wafers, obtained by pycnometry

Deposition T (K)	Anneal <sup>a</sup> T (K)	Density (g·cm <sup>-3</sup> )
523	—	2.25 ± 0.099 <sup>b</sup> (2) <sup>c</sup>
	873	2.14 (1)
	1173	2.46 (1)
643	—	2.13 ± 0.061 (2)
	773	2.15 (1)
	873	2.28 (1)
	973	2.26 (1)
	1173	2.29 ± 0.014 (2)
703	—	2.10 ± 0.085 (2)
	773	2.20 (1)
	873	2.30 (1)
	973	2.28 (1)
	1173	2.28 ± 0.057 (2)

<sup>a</sup>Each sample annealed in air for 72h.

<sup>b</sup>± 1σ.

<sup>c</sup>Number of measurements.

haps coincidentally, the films grown at 643 K showed a slightly higher deposition rate, suggesting possible relations among rapid deposition, metastability, and inhomogeneity.

IR spectra of the as-deposited and annealed CVD samples were taken and compared to the spectrum of bulk SiO<sub>2</sub> glass. There are a few subtle differences in the spectra, as will be discussed later, but there is also indication of a small amount of H<sub>2</sub>O present in the samples. To test whether such H<sub>2</sub>O content influences the measured enthalpy, calorimetry was performed on some bulk SiO<sub>2</sub> glass with known high and low OH<sup>-</sup> contents (Suprasil I, 1200 ppm OH<sup>-</sup>; Fusion 453, 0.1 ppm OH<sup>-</sup>). Transposed temperature drop and solution calorimetry experiments on Suprasil I gave results that agree very well with the values for dry silica glass. The IR spectra of the Fusion and Suprasil SiO<sub>2</sub> samples are the same (as the spectrum

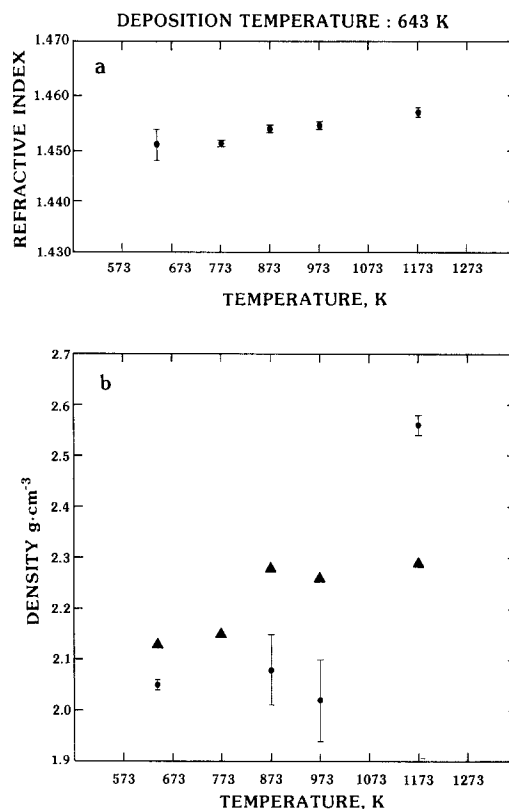


Fig. 3. a. Refractive index of LPCVD SiO<sub>2</sub> films deposited at 643 K on Si wafers vs. annealing temperature. b. Density of LPCVD SiO<sub>2</sub> films deposited at 643 K on Si wafers (circles) and stainless steel wafers (triangles) vs. annealing temperature.

of bulk SiO<sub>2</sub> glass), with the exception of the OH<sup>-</sup> absorption band for Suprasil I. Thus, it is concluded that the small amount of H<sub>2</sub>O present in the CVD samples (< 7000 ppm) is probably not the cause of the large heat effects seen.

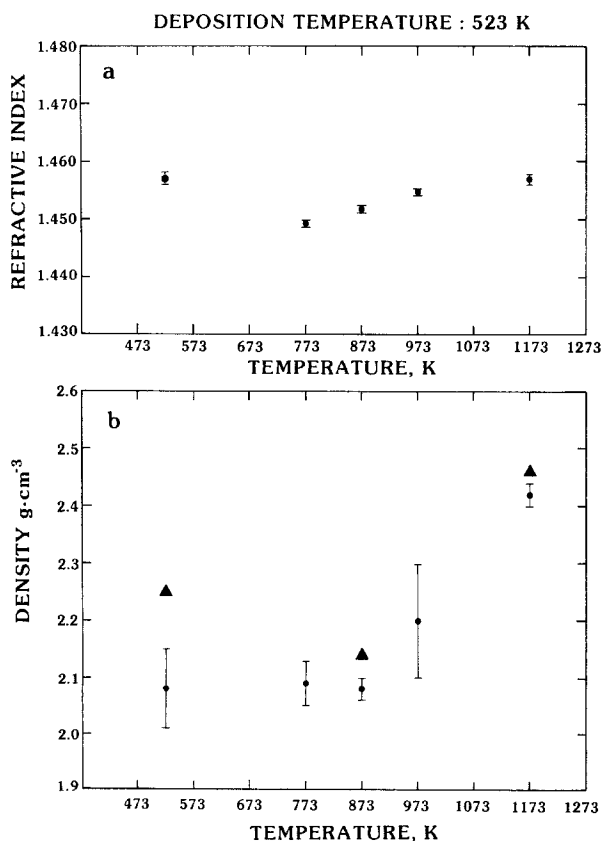


Fig. 2. a. Refractive index of LPCVD SiO<sub>2</sub> films deposited at 523 K on Si wafers vs. annealing temperature. b. Density of LPCVD SiO<sub>2</sub> films deposited at 523 K on Si wafers (circles) and stainless steel wafers (triangles) vs. annealing temperature.

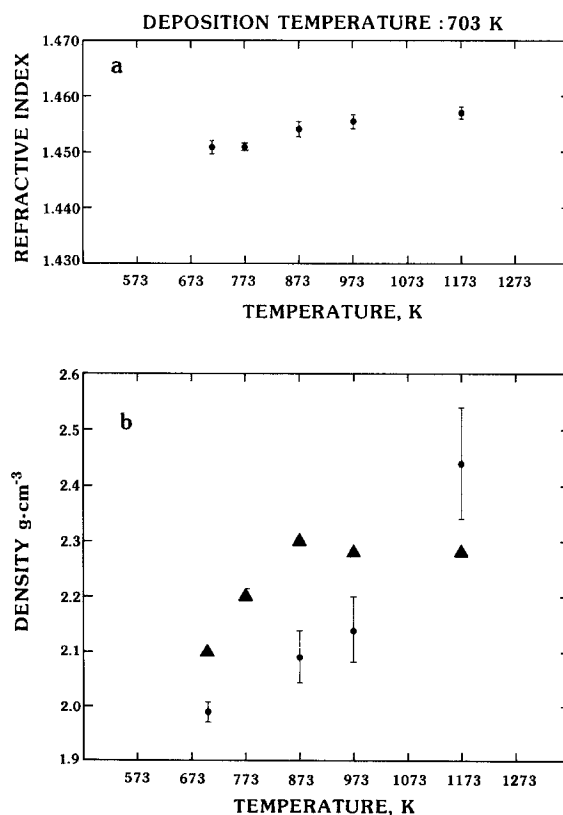


Fig. 4. a. Refractive index of LPCVD SiO<sub>2</sub> films deposited at 703 K on Si wafers vs. annealing temperature. b. Density of LPCVD SiO<sub>2</sub> films deposited at 703 K on Si wafers (circles) and stainless steel wafers (triangles) vs. annealing temperature.

**Densities and refractive indexes.**—The results from the density and refractive index measurements are listed in Tables VI and VII. Densities and refractive indexes increase as the temperature of anneal increases (see Fig. 2-4). All the circles in the figures are the means of the measurements on LPCVD film  $\text{SiO}_2$  samples collected on Si wafers, whereas the triangles are the means of the measurements on  $\text{SiO}_2$  samples collected on stainless steel wafers. The error bars attached to the circles are  $\pm 1\sigma$  (total length  $2\sigma$ ) for all the densities, thus giving a confidence interval of 95%, and  $\pm 3\sigma$  (total length of  $6\sigma$ ) for all the refractive indexes, giving a confidence interval of 99.7%.

All refractive indexes fall between 1.4500 and 1.4600 for as-deposited and annealed samples. For all three deposition temperatures, the indexes increase slightly with annealing. A general increase upon annealing is also observed in the densities of the film CVD  $\text{SiO}_2$  samples. However, the detailed behavior of the film densities may differ from that of the refractive indexes. The as-deposited samples have densities in the range 2.0-2.22  $\text{g}\cdot\text{cm}^{-3}$ , not very different from those of bulk  $\text{SiO}_2$  glass (8) and those of thermally grown  $\text{SiO}_2$  (9), or from other reported values for CVD  $\text{SiO}_2$  films (9, 10). Samples collected on stainless steel wafers are slightly more dense than the CVD films on Si wafers. For the samples deposited at 523 K, the densities of films deposited on both kinds of substrate are very similar to each other, both initially and upon annealing. For the higher deposition temperatures (643 and 703 K), the films deposited on Si appear less dense than those deposited on stainless steel. This difference persists up to the highest temperature (1173 K) on annealing. At this temperature, the  $\text{SiO}_2$  films deposited on Si show a sudden increase in density, an increase not seen in the samples grown on stainless steel. One possible explanation for this observation may be that

there was some growth of thermal oxide ( $\text{SiO}_2$ ) during the annealing in air of these samples. Such an increase, however, is seen for  $\text{SiO}_2$  films deposited on both Si and stainless steel at 523 K.

It is not clear whether these apparent differences in density trends for the various  $\text{SiO}_2$  film samples represent real structural differences. First, one must be cautious, because the uncertainties in density measurements (see error bars in Fig. 2, 3, and 4) are much larger than those in the refractive indexes. Also, densities of films deposited on Si and stainless steel were measured by different methods. Furthermore, small amounts of Fe and Cr impurities in the films deposited on stainless steel (see Table II) would tend to raise their apparent densities. Last, the difference in density of  $\text{SiO}_2$  films deposited on steel vs. those deposited on silicon could perhaps be explained on the basis of substrate temperature. Stainless steel may be hotter due to increased thermal conduction, thus leading to some densification of the film even as it is being deposited. Nevertheless, the behavior seen might suggest that the effects of deposition temperature, substrate, and annealing on film density, structure, and thermodynamics may be complex in detail, though the overall trend is toward densification and energetic relaxation with increasing temperature. The densities higher than those of bulk  $\text{SiO}_2$  glass for samples annealed at 1173 K may suggest incipient crystallization. All those samples were checked for crystals. None was found by x-ray diffraction. However, reflected light microscopy revealed a few very small islands of crystals, probably too small in overall extent to cause any substantial increase in density. However, these observations do not rule out the presence of very small microcrystalline regions present in a total concentration significant enough to affect the density. The observation that the enthalpies of solution of the samples annealed at the highest temperatures (see Table

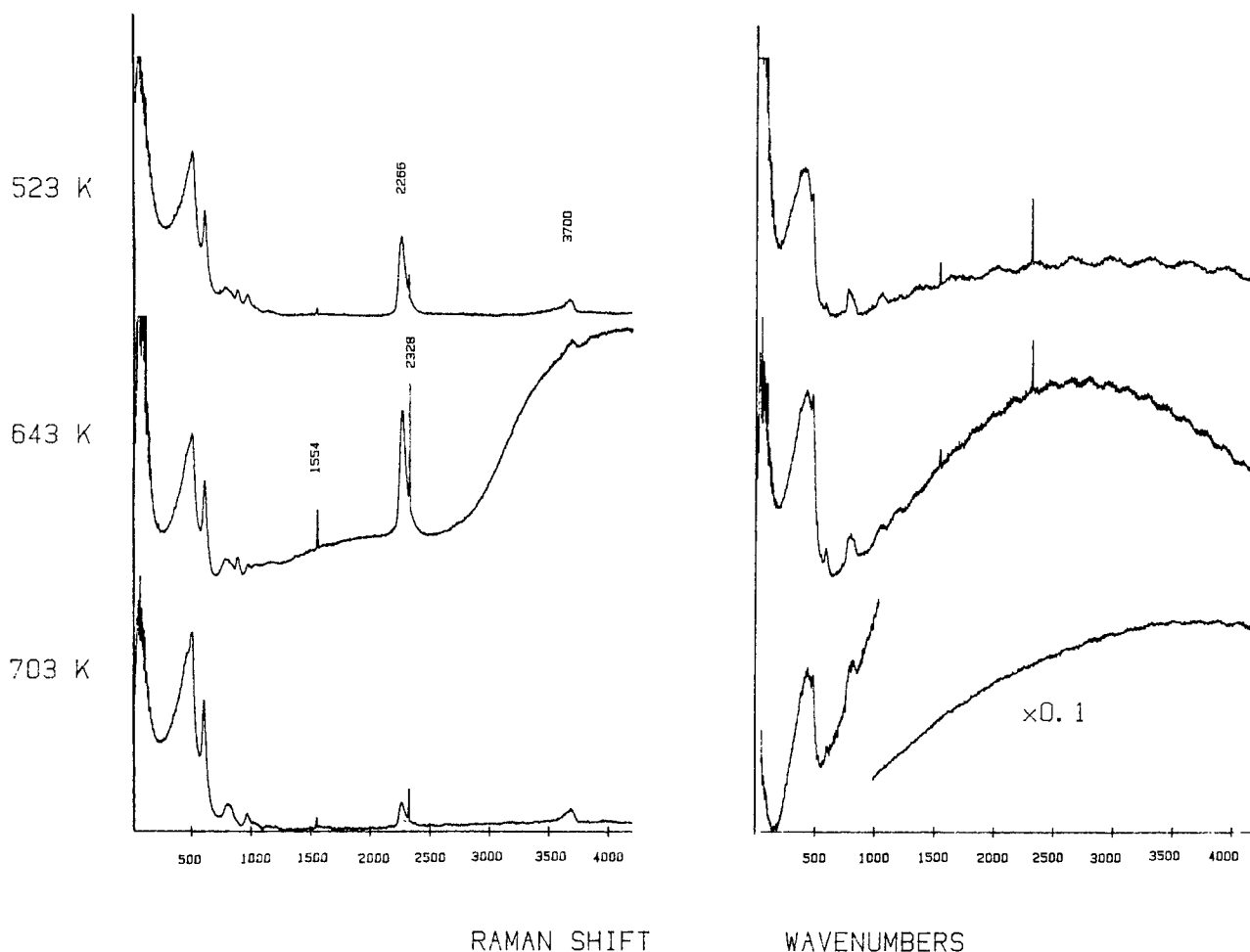
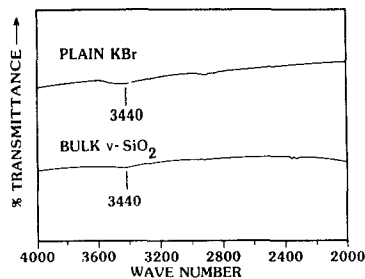


Fig. 5. Raman spectra of as-deposited (left) and annealed (right, 1173 K, ~70h) CVD  $\text{SiO}_2$  film samples



CVD SiO<sub>2</sub> FILMS

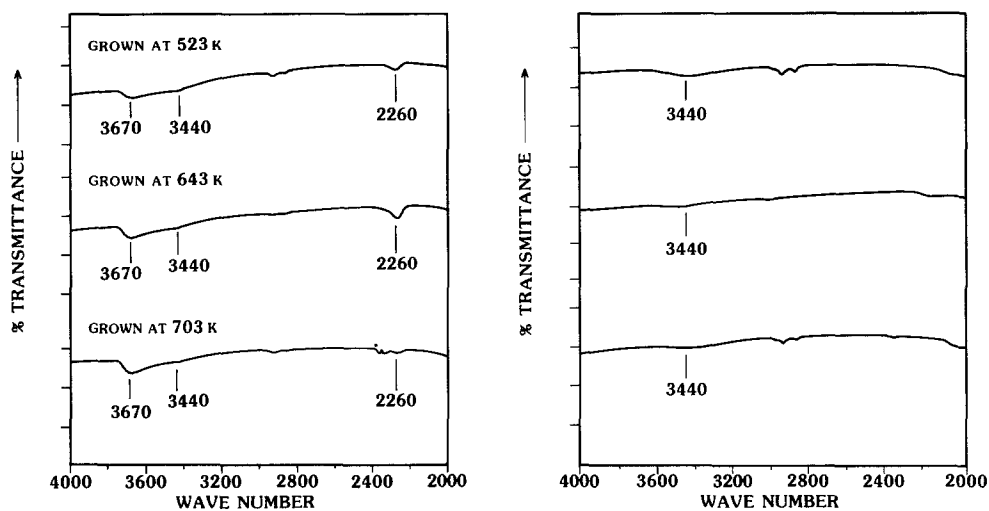
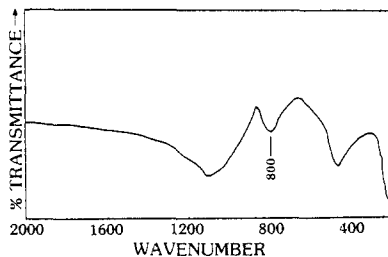


Fig. 6. Powder infrared spectra of as-deposited (left) and annealed (right, 1173 K~70h) CVD SiO<sub>2</sub> film samples from 4000-2000 cm<sup>-1</sup>. Shown at top are spectra for plain KBr disk and bulk dry vitreous SiO<sub>2</sub> in same region.

IV) tend toward values slightly less exothermic than the heat of solution of bulk silica glass also supports the idea of incipient crystallization.

It is interesting that the 523 K as-deposited film samples seem to be slightly denser than the 643 and 703 K deposited films (even after considering the errors associ-

BULK v-SiO<sub>2</sub>



CVD SiO<sub>2</sub> FILMS

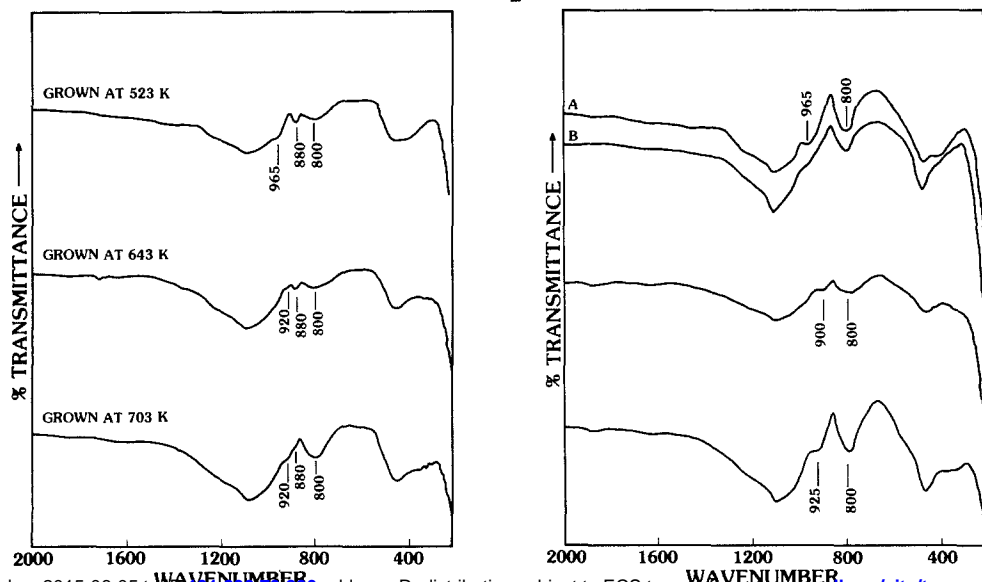


Fig. 7. Powder infrared spectra of as-deposited (left) and annealed (right, 1173 K) CVD SiO<sub>2</sub> film samples from 2000-200 cm<sup>-1</sup>. At top is spectrum of bulk dry vitreous SiO<sub>2</sub>. For 523 K annealed sample, A is spectrum after 2 days and B after 3 days of annealing, showing gradual loss of 965 cm<sup>-1</sup> band due to Si-OH species.

ated with the density measurements), for samples grown on both stainless steel and Si. The reason for this is not known, but such denser films might be technologically interesting [improved physical and/or dielectric properties (11, 12)].

**Infrared and Raman spectroscopy.**—Raman and infrared spectra of the as-deposited and annealed at 1173 K for ~70h SiO<sub>2</sub> film samples are shown in Fig. 5-7. An extended discussion can be found elsewhere (5), and only a summary is presented here.

The most important features in the Raman and infrared spectra are: bands at ~3700 and ~970 cm<sup>-1</sup> due to hydroxyl groups present as Si-OH species (13, 15) that disappear on annealing, and an asymmetric peak near 2270 cm<sup>-1</sup>, most probably due to Si-H species in the as-deposited films and snows (14). This peak disappears on annealing as well.

The Si-H relative concentration varies, with deposition temperature being lowest at the highest temperature. This might indicate a more complete reaction at higher temperatures. When the samples are annealed, both Si-OH and Si-H species disappear, probably through condensation to SiOSi linkages and elimination of H<sub>2</sub> and/or H<sub>2</sub>O. The high frequency bands shift upward from 1040 and 1160 cm<sup>-1</sup> for the as-deposited samples to 1060 and 1200 cm<sup>-1</sup> on annealing. Furthermore, the major low frequency band at 470 cm<sup>-1</sup> shifts to 430 cm<sup>-1</sup> after annealing (Fig. 5). This does not suggest that the as-deposited LPCVD samples are denser than bulk SiO<sub>2</sub> glass, but it does demonstrate that there is enough local structure change, perhaps due to Si-H and Si-OH species, for the spectra to be affected (5).

**Scanning electron microscopy.**—SEM micrographs of both film and snow CVD SiO<sub>2</sub> samples are shown in Fig.

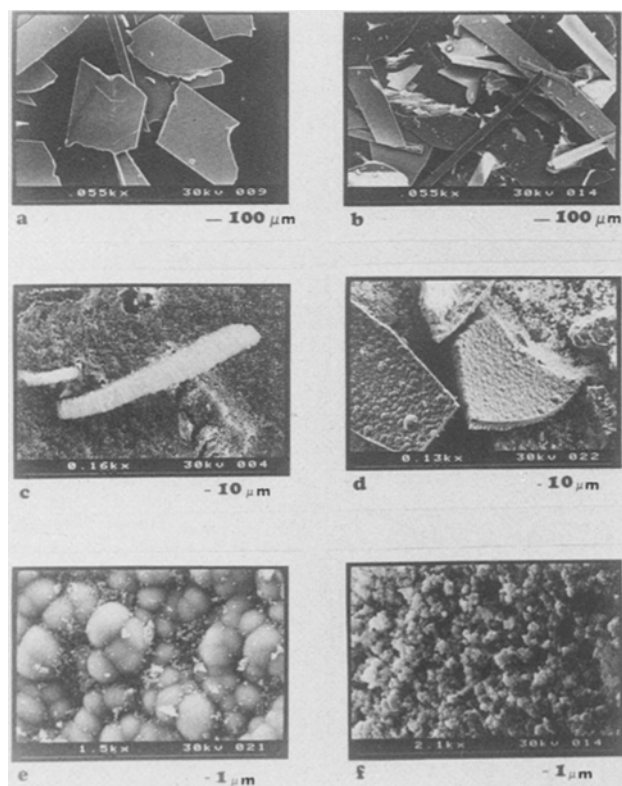


Fig. 8. a: SEM micrograph of film CVD SiO<sub>2</sub> deposited at 643 K. Overall picture. b: SEM micrograph of film CVD SiO<sub>2</sub> deposited at 523 K. c: SEM micrograph of snow CVD SiO<sub>2</sub> deposited during the 703 K run. Individual particle length ~530 μm. d: SEM micrograph of snow CVD SiO<sub>2</sub> deposited during the 703 K run, annealed at 1223 K for 72h. Bubbles are clearly seen (see text). e: SEM micrograph of snow CVD SiO<sub>2</sub> deposited during the 703 K run, annealed at 1223 K for 72h. Close up of bubbles. Diameter range from 2 to 11 μm. f: SEM micrograph of snow CVD deposited during the 703 K run, annealed at 1223 K for 72h. Close-up of the surface. See text.

8. The surface of the film samples is basically smooth with some bubbles. These bubbles may be due to traces of H<sub>2</sub> trying to escape from the samples or, possibly, due to nodules of SiO<sub>2</sub> formed in the gas phase and actually incorporated in the films. The possibility that the bubbles are formed by incorporated particulate contaminants or by some roughness of the stainless steel substrates is less likely, because the bubbles appear perfectly spherical.

The snow samples appear very different. The as-deposited sample differs remarkably from the annealed sample. In the latter, numerous bubbles can be seen, and the sample looks sintered (Fig. 8d). The diameters of the bubbles vary between ~5 and ~30 μm. Their origin is most probably due to H<sub>2</sub> gas evolution, but it is also possible that there was some gas phase nucleation due to turbulence during deposition, thus resulting in SiO<sub>2</sub> nodule formation.

We attempted to measure the surface area of the snows by using the BET method (16). A type V isotherm was obtained (16, 17), making it difficult to make any reasonable surface area measurement. Nevertheless, it is clear that the snows have a very high surface area. This can be seen in Fig. 8f, which, in addition to showing overall small particle size (0.5-1.2 μm), shows complex morphology, with each particle having a larger surface area than that of a smooth sphere of similar dimensions.

## Conclusions

High temperature drop and solution calorimetry has shown that the as-deposited LPCVD SiO<sub>2</sub> samples on stainless steel substrates are metastable by up to 101 kJ·mol<sup>-1</sup> when compared to bulk SiO<sub>2</sub> glass. This difference is large compared to the enthalpy difference between various silica polymorphs [e.g., glass, quartz, cristobalite, tridymite, and coesite (7)]. It may be related to the large surface area of the snow samples and to specific local structural differences in the silica framework due both to the conditions of deposition and also possibly to the presence of Si-H and Si-OH species in the CVD samples. These differences disappear gradually with annealing.

The refractive indexes of SiO<sub>2</sub> films deposited on stainless steel and on Si fall between 1.4500 and 1.4600 for as-deposited and annealed samples. Both densities and refractive indexes of the film samples generally increase with annealing temperature, but their detailed behavior is different. It is not clear whether apparent differences in density trends for the various SiO<sub>2</sub> films represent real structural differences.

## Acknowledgments

We would like to thank Dr. Patrick McMillan for his valuable help and comments on the spectroscopy and for the Raman spectra. Special thanks also go to Ms. Susan Selkirk for drafting the figures and to Mr. Patrick Trusty for all the SEM work. This research was supported by NSF Grant DMR 8211127. This work is part of M.H.'s Ph.D. thesis.

Manuscript submitted May 13, 1985; revised manuscript received Aug. 9, 1985. This was Paper 345 presented at the New Orleans, Louisiana, Meeting of the Society, Oct. 7-12, 1984.

Arizona State University assisted in meeting the publication costs of this article.

## REFERENCES

1. K. Soto, Y. Nishi, and T. Abe, in "Thin Film Dielectrics," F. Vratny, Editor, p. 378, The Electrochemical Society Softbound Proceedings Series, New York (1969).
2. W. Kern and A. W. Fisher, *RCA Rev.*, **21**, 715 (1970).
3. G. L. Schnable, *Solid State Technol.*, **21**, 69 (1978).
4. W. Kern and V. S. Ban, in "Thin Film Processes," J. L. Vossen and W. Kern, Editors, Chapter III-2, Academic Press, New York (1978).
5. M. Huffman and P. McMillan, *J. Non-Cryst. Solids*, To be published.
6. A. Navrotsky, *Phys. Chem. Min.*, **2**, 89 (1977).

7. P. Richet, Y. Bottinga, L. Denielou, J. P. Petitet, and C. Tequi, *Geochim. Cosmochim. Acta*, **46**, 2639 (1982); R. A. Robie, B. S. Hemingway, and J. R. Fisher, "Thermodynamic Properties of Minerals and Related Substances at 298.15 K and 1 Bar ( $10^5$  Pascals) Pressure and at Higher Temperatures," Geological Survey Bulletin 1452, Washington, DC (1978).
8. R. K. Iler, "The Chemistry of Silica," p. 19, John Wiley and Sons, New York (1979); Kirk-Othmer Encyclopedia of Chemical Technology, Vol. 20, p. 752, Wiley-Interscience, New York (1978).
9. N. Nagasima, *J. Appl. Phys.*, **43**, 3378 (1972).
10. W. Kern, *Semicon. Int.*, **5**, 89 (1982).
11. W. Kern, G. L. Schnable, and A. W. Fisher, *RCA Rev.*, **37**, 3 (1976).
12. W. Kern and R. Heim, *This Journal*, **117**, 568 (1970).
13. G. E. Walrafen and S. R. Samanta, *J. Chem. Phys.*, **67**, 4260 (1977).
14. G. H. A. M. van der Steen and H. van den Boom, *J. Non-Cryst. Solids*, **23**, 279 (1977).
15. W. A. Pliskin and P. P. Castrucci, *This Journal*, **6**, 85 (1968).
16. C. N. Satterfield, "Heterogeneous Catalysis in Practice," Chap. 5, McGraw-Hill, New York (1980).
17. S. J. Gregg and K. S. Sing, "Adsorption, Surface Area, and Porosity," Chap. 3, Academic Press, New York (1967).

## Crystal Perfection of Silicon Single Crystals Grown by the Magnetic-Field-Applied Czochralski Method

Seiji Kawado and Toshiyuki Maruyama

*Sony Corporation Research Center, 174 Fujitsuka-cho, Hodogaya-ku, Yokohama 240, Japan*

Toshihiko Suzuki, Nobuyuki Isawa, and Kinji Hoshi

*Sony Corporation, Semiconductor Group, 4-14-1 Asahi-cho, Atsugi-shi, Kanagawa 243, Japan*

### ABSTRACT

Silicon single crystals that had various oxygen concentrations and that had been grown by the magnetic-field-applied Czochralski (MCZ) method were investigated by two-step annealing to examine the defect generation associated with oxygen precipitation. The crystallinity of the crystals was characterized by x-ray anomalous transmission, IR absorption, x-ray section topography, and selective etching techniques and compared with that of conventional CZ crystals. Oxygen precipitation and defect generation were not found in MCZ crystals with oxygen concentrations less than  $5 \times 10^{17}$  at./cm<sup>3</sup>. In MCZ crystals with oxygen concentrations more than  $5 \times 10^{17}$  at./cm<sup>3</sup>, the density of defects such as oxygen precipitates, dislocation loops, and stacking faults was much less than in CZ crystals.

The magnetic-field-applied Czochralski (MCZ) method produces high quality silicon single crystals by applying a transverse magnetic field during crystal growth to suppress the turbulent convection of the melt (1-3). This method enables us to control a wider range of oxygen concentrations in silicon, to obtain higher resistivity, and to improve the radial distribution of resistivity more than was previously possible with the CZ method. The MCZ method makes possible oxygen concentrations within a range of  $0.5\text{--}12 \times 10^{17}$  at./cm<sup>3</sup> (3), while the conventional CZ method makes possible oxygen concentrations only within a range of about  $10 \times 10^{17}$  at./cm<sup>3</sup>. It is well known that oxygen in silicon is closely related to the defects generated during the high temperature processes required by device fabrication. Using two-step annealing, we have investigated dislocation-free MCZ silicon crystals with various oxygen concentrations. In this paper, we report that oxygen precipitation and defect generation are not found in MCZ crystals with low oxygen concentrations, and that MCZ crystals with high oxygen concentrations have better crystallinity than conventional CZ crystals.

### Experimental Procedure

Test samples were four groups of MCZ wafers with different oxygen concentrations, with a group of conventional CZ wafers as reference. Oxygen concentrations of

the samples are shown in Table I. The p-type (B doped) wafers had a 3 or 4 in. diameter, about a 380  $\mu\text{m}$  thickness, a (001) orientation, and a 10-15  $\Omega\text{-cm}$  resistivity. The front and back surfaces of the wafers were mechanically and chemically polished.

Crystal perfection was investigated in the as-grown state, after the first annealing and after the second annealing, using x-ray diffraction intensity measurements, x-ray section topography, and selective etching techniques, according to the flow chart shown in Fig. 1. Oxygen concentration was also measured by infrared absorption at each stage to allow a better understanding of the precipitation behavior.

*Two-step annealing.*—The samples were subjected to the first annealing in order to generate the embryos of

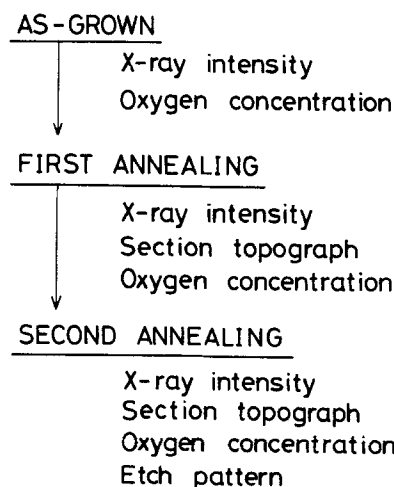


Table I. Oxygen concentration of test samples

Sample	Growth method	Oxygen concentration (at./cm <sup>3</sup> )
M-1	MCZ	$11.2 \times 10^{17}$
M-2	MCZ	$5.8 \times 10^{17}$
M-3	MCZ	$2.9 \times 10^{17}$
M-4	MCZ	$1.2 \times 10^{17}$